



Amyloid- β accumulation in relation to functional connectivity in aging: A longitudinal study

Guodong Liu^a, Chenye Shen^a, Anqi Qiu^{a,b,c,d,e,f,*}

^a Department of Biomedical Engineering, National University of Singapore, Singapore

^b NUS (Suzhou) Research Institute, National University of Singapore, China

^c The N.1 Institute for Health, National University of Singapore, Singapore

^d Institute of Data Science, National University of Singapore, Singapore

^e Department of Health Technology and Informatics, the Hong Kong Polytechnic University

^f Department of Biomedical Engineering, the Johns Hopkins University, USA

ARTICLE INFO

Keywords:

Amyloid deposition
Functional brain organization
Positron emission tomography
Resting-state fMRI
Brain aging
Functional connectivity

ABSTRACT

The brain undergoes many changes at pathological and functional levels in healthy aging. This study employed a longitudinal and multimodal imaging dataset from the OASIS-3 study ($n = 300$) and explored possible relationships between amyloid beta ($A\beta$) accumulation and functional brain organization over time in healthy aging. We used positron emission tomography (PET) with Pittsburgh compound-B (PIB) to quantify the $A\beta$ accumulation in the brain and resting-state functional MRI (rs-fMRI) to measure functional connectivity (FC) among brain regions. Each participant had at least 2 to 3 follow-up visits. A linear mixed-effect model was used to examine longitudinal changes of $A\beta$ accumulation and FC throughout the whole brain. We found that the limbic and frontoparietal networks had a greater annual $A\beta$ accumulation and a slower decline in FC in aging. Additionally, the amount of the $A\beta$ deposition in the amygdala network at baseline slowed down the decline in its FC in aging. Furthermore, the functional connectivity of the limbic, default mode network (DMN), and frontoparietal networks accelerated the $A\beta$ propagation across their functionally highly connected regions. The functional connectivity of the somatomotor and visual networks accelerated the $A\beta$ propagation across the brain regions in the limbic, frontoparietal, and DMN networks. These findings suggested that the slower decline in the functional connectivity of the functional hubs may compensate for their greater $A\beta$ accumulation in aging. The $A\beta$ propagation from one brain region to the other may depend on their functional connectivity strength.

1. Introduction

The brain undergoes many changes at pathological levels in healthy aging. Pathological changes in the brain with aging include the accumulation of amyloid beta ($A\beta$) and neurofibrillary tangles (tau), which are associated with Alzheimer's disease. The $A\beta$ accumulation occurs while individuals are still cognitively normal (Bennett et al., 2006; Price and Morris, 1999), decades before AD symptoms appear, emphasizing the importance of healthy aging research to detect early $A\beta$ deposition (Karran et al., 2011).

Positron emission tomography (PET) with Pittsburgh compound-B (PIB) has been widely used to examine amyloid accumulation in the brain (Quigley et al., 2011). Previous studies found an increase in the $A\beta$ accumulation of the whole brain with aging (Jack et al., 2009; Sojkova et al., 2011; Villemagne et al., 2011). The $A\beta$ is more likely to aggregate in some regions of the brain before spreading throughout

the neocortex and causing neurodegeneration (Braak and Braak, 1991; Thal et al., 2002). Greater $A\beta$ accumulation was found in the posterior cingulate cortex (PCC), precuneus (Palmqvist et al., 2017; Rodrigue et al., 2012), and the temporal and frontal cortices (Sojkova et al., 2011; Villain et al., 2012). These regions have been highlighted as functional hubs in the brain that are the center of brain communication and neural integration (van den Heuvel and Sporns, 2013). It is suggested that regions vulnerable to $A\beta$ accumulation are highly functionally interconnected (Jagust and Mormino, 2011). Further research is needed to fully understand this relationship and to identify potential interventions that may help to reduce $A\beta$ accumulation and improve functional brain organization in older adults.

Cross-sectional studies mainly restricted the regions at the default mode network (DMN) and showed that greater DMN functional connectivity (FC) was associated with the elevated $A\beta$ accumulation level (Hahn et al., 2019; Jagust and Mormino, 2011; Lim et al., 2014). Also,

* Corresponding author at: Department of Biomedical Engineering, National University of Singapore, 4 Engineering Drive 3, Block E4 #04-08, Singapore 117583, Singapore.

E-mail address: anqi.qiu.sg@gmail.com (A. Qiu).

<https://doi.org/10.1016/j.neuroimage.2023.120146>.

Received 15 January 2023; Received in revised form 11 April 2023; Accepted 28 April 2023

Available online 29 April 2023.

1053-8119/© 2023 The Authors. Published by Elsevier Inc. This is an open access article under the CC BY-NC-ND license (<http://creativecommons.org/licenses/by-nc-nd/4.0/>)

Table 1
Clinical and demographic characteristics.

	All included subjects (<i>n</i> = 300)	Subjects with longitudinal fMRI (<i>n</i> = 258)	Subjects with longitudinal PET (<i>n</i> = 141)	Subjects with both longitudinal fMRI and PET (<i>n</i> = 89)	Statistics for Group comparisons
gender (M/F)	118/182	107/151	45/96	34/55	$\chi^2 = 3.63$
baseline age, year	65.9 (8.8)	66.3 (8.4)	64.4(9.0)	65.4(7.9)	$F_{3,784} = 1.74$
education, year	16.0 (2.5)	16.0 (2.5)	15.9(2.5)	15.9(2.6)	$F_{3,784} = 0.09$
MMSE	29.2(1.1)	29.1(1.2)	29.2(1.2)	29.1(1.4)	$F_{3,784} = 0.35$
number of visits	2.7 (0.9)	2.6 (0.9)	2.4(0.6)	2.2(0.6)	–
duration of the first and last scans, year	4.9 (2.3)	4.8 (2.1)	4.9(2.3)	4.7(1.9)	–

Abbreviations: M, male; F, female; MMSE, mini-mental state examination. All $p > 0.05$.

Elman et al. (2014) examined the relationship between voxel-wise brain FC and $A\beta$ accumulation in the frontoparietal, salience, and dorsal attention networks in healthy aging. Such a relationship has been explained as a compensatory mechanism that the increased FC compensated for the $A\beta$ pathology (Lim et al., 2014; Mormino et al., 2011). However, it is important to note that cross-sectional studies can only observe correlations between $A\beta$ accumulation and functional connectivity and cannot establish causation. Therefore, longitudinal studies would help determine whether $A\beta$ accumulation leads to changes in functional connectivity or if functional connectivity precedes or contributes to changes in $A\beta$ accumulation.

This study employed a longitudinal and multimodal imaging dataset from the OASIS-3 study. We explored 1) the longitudinal relationship between the $A\beta$ accumulation and functional connectivity in the whole brain, 2) whether the $A\beta$ pathology influences functional brain organization over time, and 3) whether the $A\beta$ propagation over time is related to brain functional wiring. We hypothesized that functional hub regions, such as the PCC and precuneus, would exhibit a higher rate of $A\beta$ accumulation but a slower decline in functional connectivity in healthy aging, supporting the compensatory mechanism. Moreover, we expected that $A\beta$ accumulation might propagate along possible pathways of functional hubs over time. The study computed participation coefficients (PC) to quantify which brain regions play a hub role in connecting to the brain subnetworks (Bertolero et al., 2018; Power et al., 2013). This study, to the best of our knowledge, provided understanding of the longitudinal relationship between $A\beta$ and FC in healthy aging.

2. Methods

2.1. Participants

This study employed the image data from the OASIS-3 cohort (<https://www.oasis-brains.org>). The OASIS-3 included 1098 participants aged from 42 to 95 collected across several ongoing studies in the Washington University Knight Alzheimer Disease Research Center throughout 15 years (LaMontagne et al., 2019). All participants signed informed consent for the OASIS-3 imaging study.

Fig. 1 illustrates the flowchart of the participant selection. In brief, the OASIS-3 study included 605 cognitively normal participants. This study included 300 cognitively normal participants with longitudinal functional MRI or/and PIB-PET data. Among them, 141 participants had longitudinal PIB-PET data, 265 participants had longitudinal fMRI data. Only 258 subjects have good fMRI data. Among them, 89 participants had both longitudinal fMRI and PIB-PET data. Table 1 lists the demographical and clinical information of the participants.

2.2. MRI acquisition and processing

The OASIS-3 study performed structural T_1 -weighted MRI and resting-state fMRI on SIEMENS Trio 3T MRI or Biograph mMR (PET/MR) 3T scanners. The image acquisition was detailed in <http://www.oasis-brains.org/#data>.

2.2.1. Structural T_1 -weighted MRI

FreeSurfer longitudinal analysis pipeline was used to label each voxel in the T_1 -weighted image as gray matter, white matter, cerebrospinal fluid (CSF), or subcortical structures (Fischl et al., 2002). Post-processing quality check was conducted following the instruction on <https://surfer.nmr.mgh.harvard.edu/fswiki/FsTutorial/TroubleshootingData>. The FreeSurfer longitudinal pipeline created a within-subject structural template to represent the subject's anatomy. Large deformation diffeomorphic metric mapping (LDDMM) to align these subjects' templates to the JHU MNI atlas (Du et al., 2011; Tan and Qiu, 2016; Zhong, 2010).

2.2.2. Resting-state fMRI (rs-fMRI)

Rs-fMRI were preprocessed in FSL with slice timing, zero padding, motion correction, skull stripping, and intensity normalization (Smith et al., 2004). Only the scans with mean framewise displacement (FD) less than 0.5 mm and had 5% of the time-series volume with FD less than 0.5 mm were included. Fig. S1 in the Supplementary Material illustrates the distribution of FD among the participants used in this study. The whole brain, white matter, and cerebrospinal fluid (CSF) signals with six motion parameters were regressed and band-pass filtered (0.01–0.08 Hz). For each participation, the rs-fMRI scan was transformed to the within-subject T_1 -weighted image via a boundary-based registration method (Greve and Fischl, 2009) and then to the JHU MNI atlas via the transformation obtained from its corresponding T_1 -weighted image and the atlas image.

This study used a whole-brain parcellation with 268 brain regions of interest (ROIs) (Shen et al., 2013). We employed the GLASSO algorithm on ROI's fMRI time series to estimate a functional connectivity matrix (268 × 268) (Colclough et al., 2018; Qiu et al., 2015). The GLASSO is a sparse inverse covariance estimation approach for computing functional connectivity matrices. It can avoid an indirect functional connection between regions A and C if both are functionally connected with region B. This approach has been used for better estimation of the functional connectivity matrix and elucidating brain functional networks in aging (Colclough et al., 2018; Qiu et al., 2015). This study employed this approach because the functional connectivity estimation would not spit over the relationship between the functional connectivity and the $A\beta$ SUVR accumulation from region A to C due to their indirect functional connection.

We further computed participation coefficients (PC) from the functional connectivity matrix to represent the diversity of intermodular connections of brain regions (Bertolero et al., 2018). The higher PC indicates that the ROI is a functional hub connecting the brain sub-networks (Power et al., 2013). This study employed this metric to interpret the hub role of brain regions.

For visualization, this study further clustered the 268 ROIs into seven functional cortical networks based on Yeo's atlas (Yeo et al., 2011) and four subcortical networks. The seven cortical networks are visual, somatomotor, dorsal attention, ventral attention, limbic, frontoparietal, default mode. The four subcortical networks include the cerebellum,

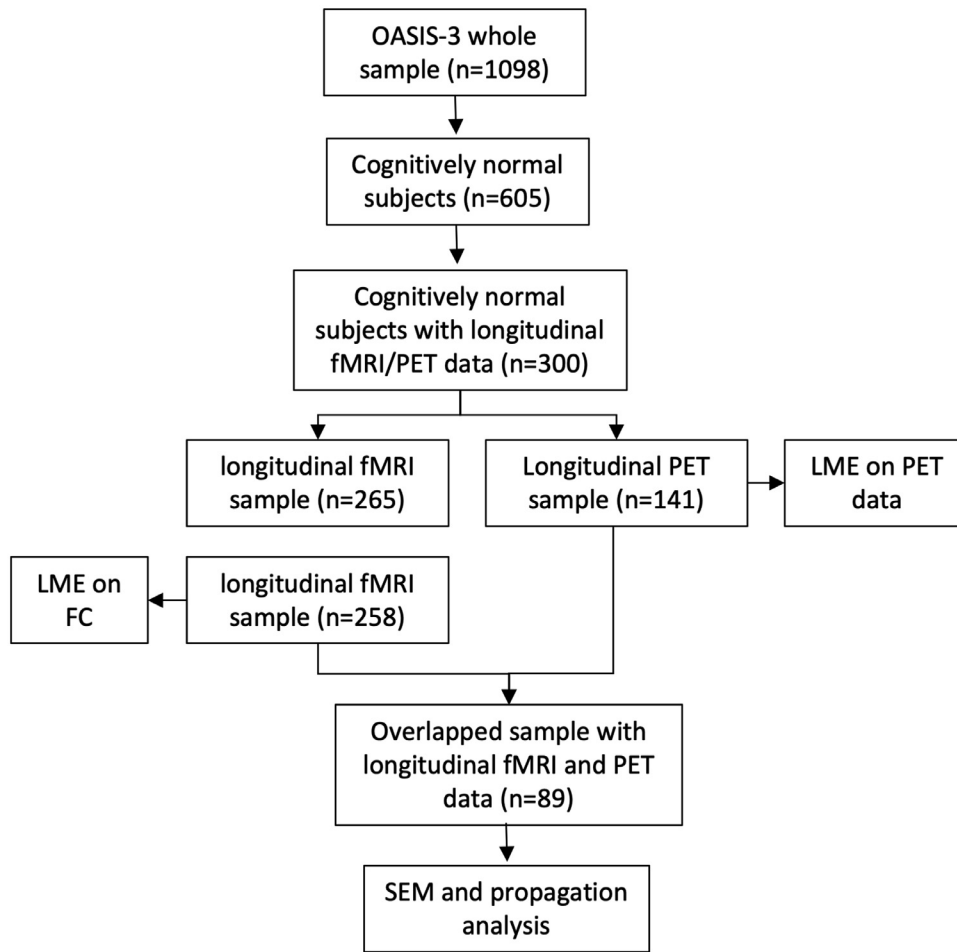


Fig. 1. The flowchart of the participant selection and statistical analysis of each dataset.

subcortical (basal ganglia and thalamus), medial temporal lobe (MTL, hippocampus), and amygdala (left and right amygdala) networks. Fig. S2 in the Supplementary Material illustrates the brain functional parcellation.

2.3. PIB-PET acquisition and processing

PET scans were performed on Biograph mMR (PET/MR), 40 PET/CT, and ECAT HRplus 962 PET scanners. This study only employed Pittsburgh Compound B ([¹¹C]PIB or PIB) PET scans (PIB-PET). The acquisition and procedure of PIB-PET were detailed at <http://www.oasis-brains.org/#data>.

This study employed PET unified pipeline (PUP) to analyze the PIB-PET data (Su et al., 2015, 2013). PET images were first smoothed to obtain a typical spatial resolution of 8 mm to harmonize them across PET scanners (Joshi et al., 2009). Standard image registration tools were used to conduct inter-frame motion correction for dynamic PIB-PET data (Eisenstein et al., 2012; Hajnal et al., 1995). Vector-gradient algorithm (VGM) was utilized to register PET to MR in a symmetric fashion (Rowland et al., 2005). Partial volume effects (PVE) were corrected based on a regional spread function (RSF) technique (Rousset et al., 2008, 1998) to improve PET quantification and obtain improved sensitivity to longitudinal changes in amyloid load (Su et al., 2016, 2015).

The peak time window of 30–60 min after injection was chosen for PIB-PET analysis. A regional target-to-reference intensity ratio, known as a standard uptake ratio (SUVR), was calculated at each voxel when the cerebellum was used as a reference.

2.4. Statistical analysis

First, we conducted a linear mixed-effects model (LME) to examine the longitudinal trajectory of $A\beta$ or FC in each ROI. The model is given below:

$$Y_{ij} = \beta_1 + \beta_2 t_{ij} + \beta_3 Gender_i + \beta_4 Education_i + \beta_5 BslAge_i + b_{1i} + b_{2i} t_{ij} + e_{ij} \quad (1)$$

i and j denoted the indices of subjects and time points, respectively. Y_{ij} was the SUVR value or functional connectivity at time t_{ij} . We defined t_{ij} as the time interval between the j_{th} follow-up scan and the age at the baseline scan ($BslAge_i$). Here, each subject's baseline was defined as the first useable time point. Gender and education were considered as covariates since the education level was found to be a risk factor for AD ((Qiu et al., 2001), and male and female brain sizes differed (Ritchie et al., 2018). The mean framewise displacement of head motion in fMRI images was considered an additional covariate for FC. β_1 to β_5 represented fixed effects, while b_{1i} , b_{2i} represented random effects that modeled the individual-specific intercept and accumulation rate of subject i . False discovery rate (FDR) (Benjamini and Hochberg, 1995) was used for the correction of multiple comparisons at a significance level of 0.05. When Y_{ij} was the SUVR value, the sample size for the LME analysis was 141. In contrast, when Y_{ij} was the FC value, the sample size for the analysis was 258.

Second, we employed structural equation modeling (SEM) to examine whether the $A\beta$ level at baseline or its annual accumulation rate could influence FC and its annual change in each functional network. For this, we employed a subject-specific linear regression model as fol-

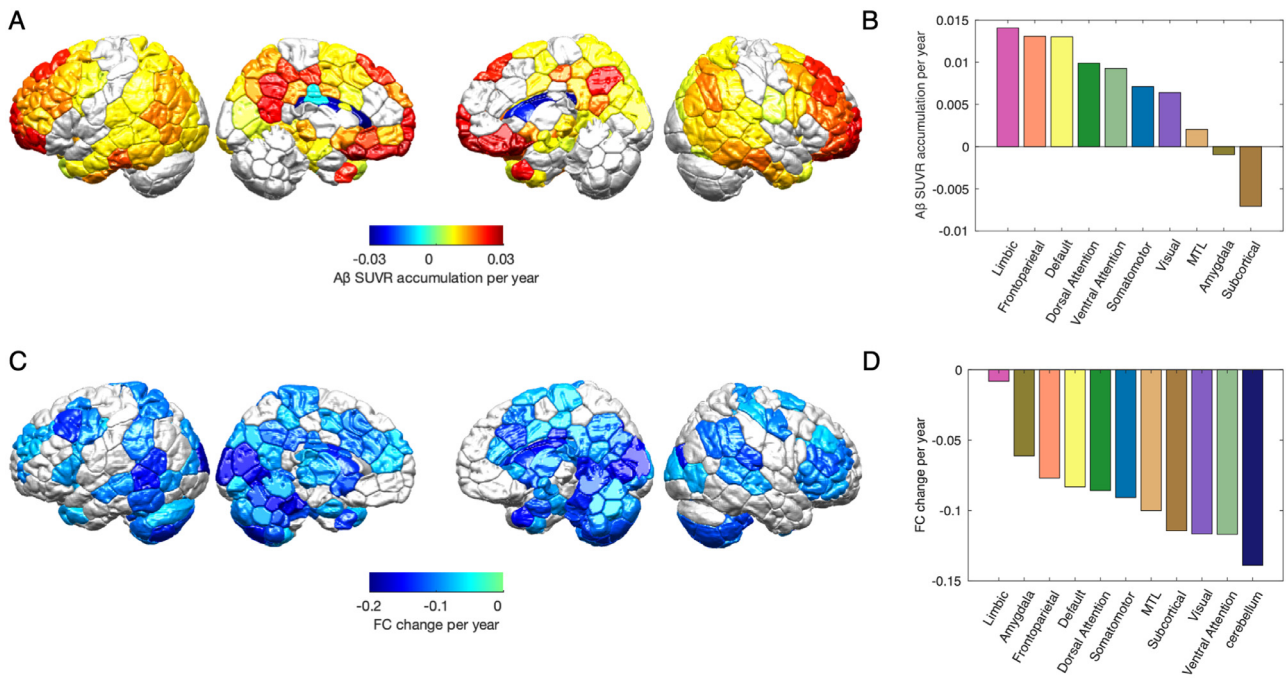


Fig. 2. Annual rates of the A β SUVR accumulation and functional connectivity (FC) at the levels of regions of interest (A, C) and functional networks (B, D). On panels A and C, regions colored in grey did not show significant annual rates at the level of FDR corrected $p < 0.05$.

lows to get the network-wise subject-specific baseline and slope of SUVR or FC:

$$Y_j = b_1 \text{Age}_j + b_2 + \varepsilon, \quad (2)$$

where j denoted j -th time point. Y_j is the functional connectivity averaged over the brain region in one functional network. b_1 was the estimated slope for A β accumulation or FC at the network level. b_2 was the estimated subject-specific baseline value at the network level. SEM was then applied to establish the paths from the SUVR baseline and slope to the FC baseline and slope. Gender, years of education, and age at baseline were included as covariates in all the paths. Since both the fMRI and PET data were used in the SEM, the sample size was 89.

Finally, we examined whether the functional connectivity of specific functional networks at baseline facilitates the spread of the A β accumulation over time. The sample size for this was 89. To test this hypothesis, we created the FC profile for each network that represents its FC to the remaining brain ROIs and was averaged over 89 participants. We then employed Pearson's correlation between the A β accumulation rate (averaged over 89 participants) and the network profile over the rest of the brain regions. Notably, only the ROIs with increased A β accumulation over time were included in this analysis. FDR (Benjamini and Hochberg, 1995) was used for the correction of multiple comparisons at a significance level of 0.05.

3. Results

3.1. Demographics

This study included 300 healthy aging participants with longitudinal MRI or PIB-PET data. Of these participants, 258 had longitudinal fMRI data, 141 had longitudinal PIB-PET data, and 89 had longitudinal fMRI and PIB-PET data. Table 1 lists gender, years of education, MMSE, the number of visits, and the duration between the first and last visits. The four datasets did not show differences in the proportion of males and females ($\chi^2 = 3.63, p > 0.05$), years of education ($F_{3,784} = 0.09, p > 0.05$),

MMSE scores ($F_{3,784} = 0.35, p > 0.05$) and baseline age ($F_{3,784} = 1.74, p > 0.05$).

3.2. Longitudinal trajectories of A β accumulation and FC in aging

Fig. 2 illustrates the averaged maps of the A β accumulation and FC annual rates across all the participants. These annual rates were survived at FDR corrected $p < 0.05$. The LME model found an increase in the A β accumulation in most of the 268 brain regions over time, particularly in the precuneus, posterior cingulate cortex (PCC), superior frontal cortex (SFC), and ventromedial prefrontal cortex (vmPFC). They were mainly located in the limbic, frontoparietal, and DMN networks (Fig. 2B).

The LME model also found a decrease in FC in most of the 268 brain regions, particularly in the ventral attention, visual, cerebellar, and subcortical networks. Figs. S3 and S4 in the Supplementary Material also illustrate individual participant data on the trajectories of the A β accumulation and FC trajectories over time, respectively.

The annual rates of the A β accumulation and FC (Fig. 1A and 1C) were significantly correlated ($r = 0.210, p < 0.001$) over all the brain regions, indicating that the higher rate of the A β accumulation was associated with a slower decline of FC.

This study further examined whether brain regions with the fastest A β accumulation and FC changes over time are functional hubs quantified by greater participation coefficients. Fig. 3A illustrates the spatial pattern of the participation coefficient across the whole brain, indicating the brain regions in the limbic, frontoparietal, and DMN networks with the greatest participation coefficient value, which was consistent with existing literature (Tomasi and Volkow, 2012). Pearson's correlation revealed that the greater participation coefficient corresponds to the faster A β SUVR accumulation ($r = 0.16, p = 0.04$; Fig. 3B) and slower FC decline over time ($r = 0.28, p < 0.001$; Fig. 3C). These findings suggested that the functional hubs may be particularly vulnerable to the annual accumulation of A β but may be able to compensate for this by maintaining strong FC. This may have implications for understanding the role of A β and FC in aging.

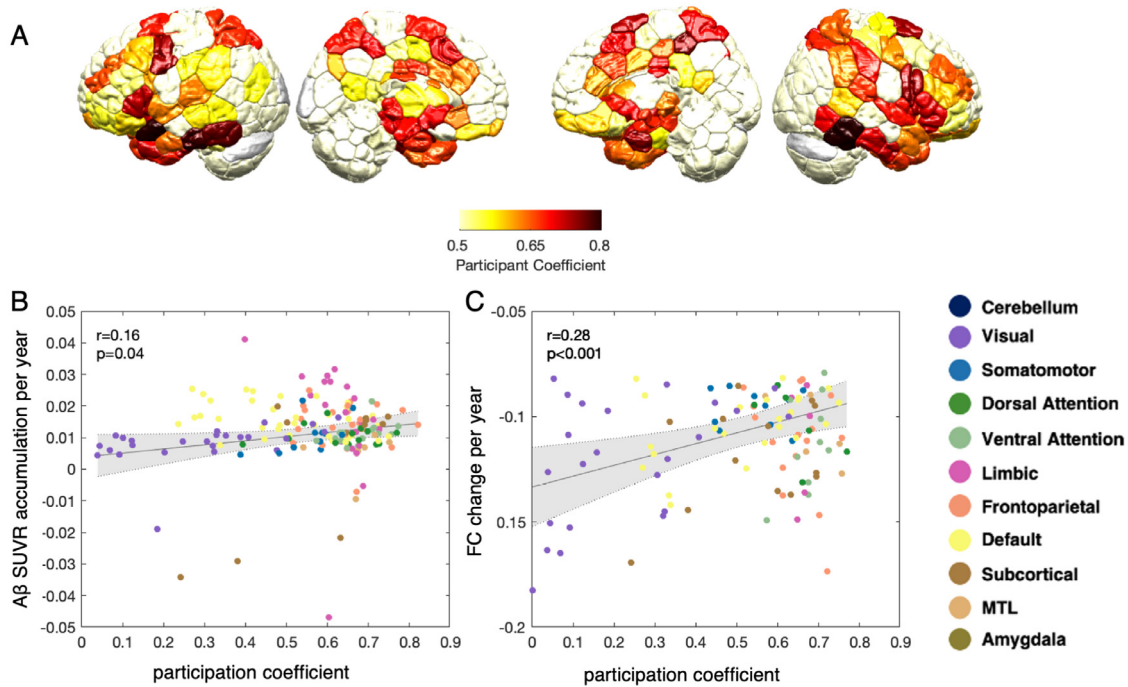


Fig. 3. Relations of participation coefficient with the annual rates of the $A\beta$ SUVR accumulation and functional connectivity (FC). Panel (A) illustrates the spatial pattern of the participation coefficient that characterizes the diversity of intermodular connections of each brain region. Panels (B, C) show the scatter plots of the participation coefficient with the $A\beta$ SUVR accumulation and FC, respectively. Each dot represents one brain region and is colored based on the functional network that it belongs to. Only the brain regions with significant annual rates of the $A\beta$ SUVR accumulation or FC are shown.

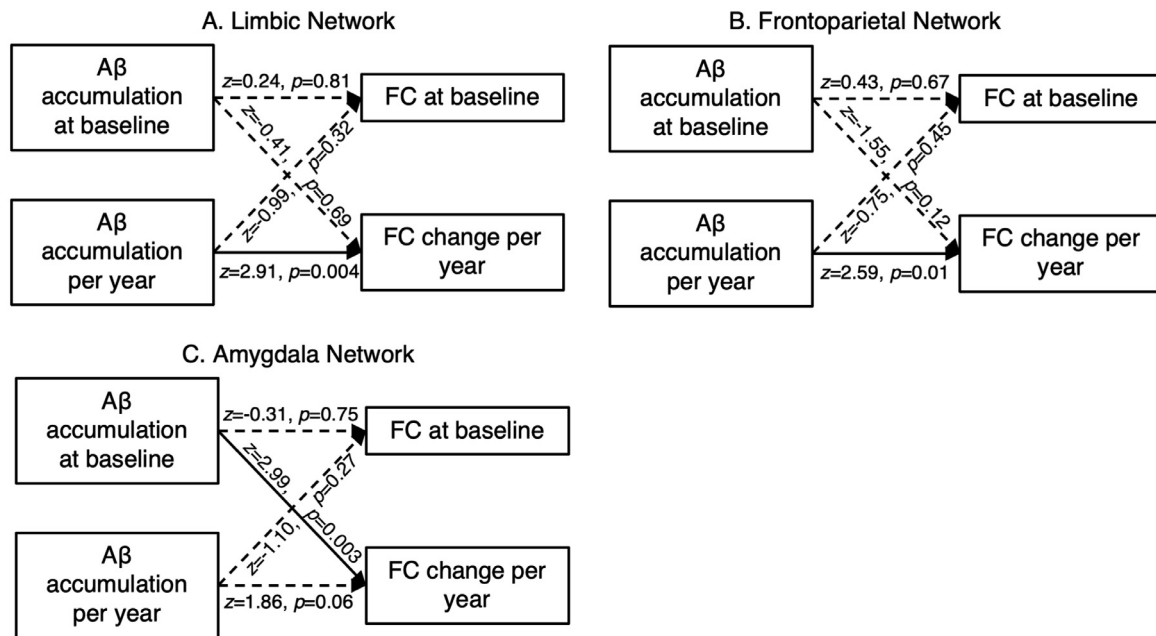


Fig. 4. Pathways demonstrate whether the $A\beta$ pathology influences brain functional connectivity (FC) over time. Panels (A-C) respectively show the pathways for the limbic, frontoparietal, and amygdala networks. Solid lines indicate significant pathways, while dashed lines indicate non-significant pathways.

3.3. $A\beta$ accumulation influences the degeneration of brain functional organization in aging

The study employed the SEM model to examine whether the $A\beta$ pathology influences the functional brain organization over time. The study revealed the positive association between the annual $A\beta$ accumulation rate and FC changes in the limbic (Fig. 4A; $z = 2.91, p = 0.004$)

and frontoparietal networks (Fig. 4B; $z = 2.59, p = 0.01$). This suggested that a greater $A\beta$ accumulation per year slows down the decline in FC in these two networks. Additionally, Fig. 4C shows that the greater $A\beta$ accumulation at baseline increases the steeper change of the FC in the amygdala network. These findings suggest that $A\beta$ pathology may have an impact on functional connectivity and its changes over time.

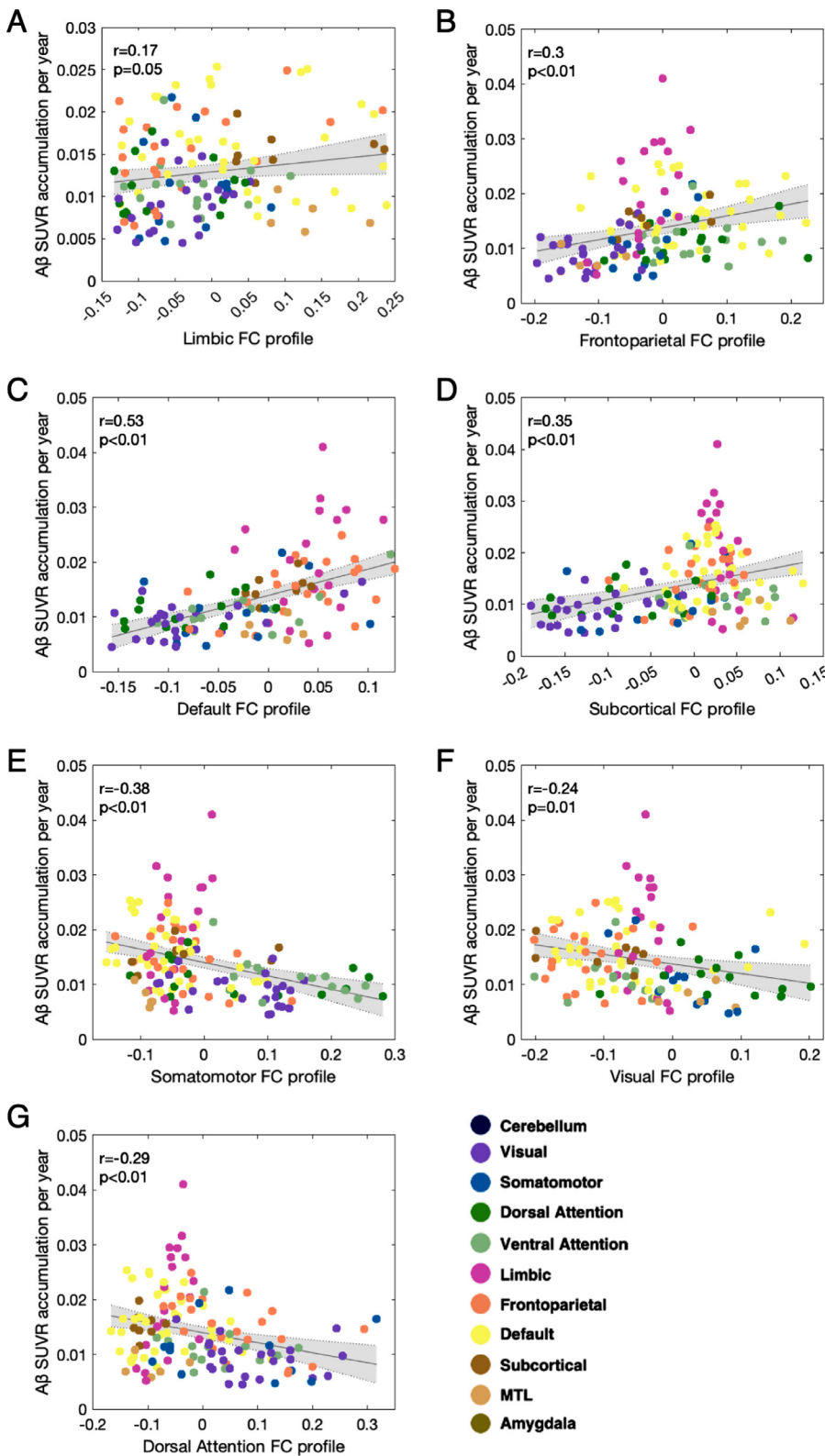


Fig. 5. The $A\beta$ accumulation propagation in relation to functional connectivity. Each panel illustrates the functional connectivity of a specific functional network with each ROI as the x-axis and the $A\beta$ accumulation change per year in each ROI as the y-axis. Only the brain regions with significant annual rates of the $A\beta$ SUVR accumulation are shown. The color indicates the functional network the ROI belongs to.

3.4. Trans-neuronal propagation of $A\beta$ accumulation

The study further examined whether the functional connectivity of each functional network at baseline facilitates the spread of the $A\beta$ accumulation over time. The study found that the functional connectivity of the limbic (Fig. 5A; $r = 0.17$, $p = 0.05$), frontoparietal (Fig. 5B; $r = 0.30$,

$p < 0.01$), DMN (Fig. 5C; $r = 0.53$, $p < 0.01$), and subcortical networks (Fig. 5D; $r = 0.35$, $p < 0.01$) at baseline was positively correlated with the annual $A\beta$ accumulation rate in the brain regions within these four networks and high-order functional networks. Additionally, the somatomotor (Fig. 5E; $r = 0.38$, $p < 0.01$), visual (Fig. 5F; $r = 0.24$, $p = 0.01$), and dorsal attention networks (Fig. 5G; $r = 0.29$, $p < 0.01$) showed that

their greater negative functional connectivity at baseline was related to the greater annual $A\beta$ accumulation rate in the brain regions of the limbic, frontoparietal, and DMN. These findings suggest that the accumulation of $A\beta$ may propagate over time through the functional pathways of the high-order functional networks.

4. Discussion

The study employed the longitudinal imaging dataset from the OASIS-3 study and investigated the relationship between the $A\beta$ accumulation and functional brain organization over time in aging. Our findings revealed that the limbic and frontoparietal networks had a greater annual $A\beta$ accumulation and a slower decline in FC in aging. Additionally, the amount of the $A\beta$ deposition in the amygdala network at baseline slowed down the decline in its FC in aging. Furthermore, the functional connectivity of the limbic, DMN, and frontoparietal networks at baseline accelerated the $A\beta$ propagation over time across their functionally highly connected regions. The functional connectivity of the somatomotor and visual networks accelerated the $A\beta$ propagation across the brain regions in the limbic, frontoparietal, and DMN networks. These findings suggested that the $A\beta$ propagation from one brain region to the other may depend on their functional connectivity.

The study found that certain brain regions, known as functional hubs, had a higher $A\beta$ accumulation rate. These functional hubs included the precuneus, PCC, and vmPFC in the DMN, and the SFC in the frontoparietal network. Previous studies have found an increase in the $A\beta$ accumulation with age in these regions (Moffat et al., 2022; Rodrigue et al., 2012; Villain et al., 2012). These findings suggested that these hub regions may be particularly vulnerable to the effects of brain aging pathology.

The study also found that an increase in the $A\beta$ accumulation rate in the limbic and frontoparietal networks and the amount of $A\beta$ in the amygdala at baseline reduced a decline in the FC change of these networks over time. This is supported by previous cross-sectional studies, which have found that the higher levels of the $A\beta$ deposition in the DMN and frontoparietal networks were associated with higher levels of functional connectivity (Elman et al., 2014; Hahn et al., 2019; Jagust and Mormino, 2011; Lim et al., 2014). The functional hubs of the limbic and frontoparietal networks have high activity and metabolism (Buckner et al., 2009). Previous research suggested that the processing of amyloid precursor protein, which can be converted into $A\beta$, may be activity-dependent, with increased $A\beta$ deposition being related to increased neuronal activity in the brain (Cirrito et al., 2005; Nitsch et al., 1993). Together, these findings suggested that the $A\beta$ pathology may help to protect against the FC decline in aging, particularly in the functional hubs of the limbic and frontoparietal networks.

Previous research was mainly based on cross-sectional data and suggested that the levels of the $A\beta$ accumulation in individual brain regions were positively related to their FC strength with the DMN (e.g., precuneus) (Sintini et al., 2020) and frontoparietal network (e.g., inferior frontal cortex) (Jones et al., 2016; Mutlu et al., 2017). This study added new evidence that the $A\beta$ propagation over time was guided by the FC strength of the high-order functional networks (e.g., the limbic, frontoparietal, and DMN) at baseline in these networks as well as the somatomotor and visual networks. These relationships between the FC and $A\beta$ are complex and not fully understood. The extracellular matrix (ECM), a network of proteins and other molecules that surround cells and help to provide structural support and regulate cell behavior, may play key roles in linking the FC and $A\beta$ in the brain. The ECM has been found to help maintain neuronal connections, which are necessary for functional connectivity (Bikbaev et al., 2015). Changes in the ECM have also been linked to changes in functional connectivity in the brain (Quattromani et al., 2018). Additionally, the ECM promotes the formation of amyloid beta plaques, and the presence of $A\beta$ plaques has been associated with changes in the ECM (Rahman and Lendel, 2021; Sun et al., 2021). Therefore, changes in the ECM may contribute to the

changes in neural connectivity and the formation of amyloid plaques. Further research is needed to fully elucidate the mechanisms underlying the relationship between the EMC, FC, and $A\beta$ in the aging brain.

There were several strengths in this study, such as the use of longitudinal and multimodal imaging data, as well as multivariate analysis. Nevertheless, the study had a limited number of participants with both longitudinal PIB-PET and fMRI images. Larger sample sizes can increase the statistical power of the study, which helps to increase the reliability and generalizability of our findings.

In conclusion, the study provided insight into the relationship between the $A\beta$ accumulation and functional brain organization, suggesting possible neural mechanisms underlying healthy aging. Further research is needed to better understand the complex interactions between $A\beta$ accumulation, functional brain organization, and cognitive function in aging.

Data and code availability

The data in this study is publicly available at <https://www.oasis-brains.org>.

Declaration of Competing Interest

No author has competing interest.

Data availability

The data sharing link is provided.

Acknowledgments

This research/project is supported by the Singapore Ministry of Education (Academic research fund Tier 1) and the National Research Foundation, Singapore and the Agency for Science Technology and Research (A*STAR), Singapore, under its Prenatal/Early Childhood Grant (Grant No. H22POM0007). The A*STAR Computational Resource centre also supported this research through the use of its high-performance computing facilities.

Supplementary materials

Supplementary material associated with this article can be found, in the online version, at [doi:10.1016/j.neuroimage.2023.120146](https://doi.org/10.1016/j.neuroimage.2023.120146).

References

- Benjamini, Y., Hochberg, Y., 1995. Controlling the false discovery rate: a practical and powerful approach to multiple testing. *J. R. Stat. Soc.: Ser. B (Methodol.)* 57, 289–300.
- Bennett, D.A., Schneider, J.A., Arvanitakis, Z., Kelly, J.F., Aggarwal, N.T., Shah, R.C., Wilson, R.S., 2006. Neuropathology of older persons without cognitive impairment from two community-based studies. *Neurology* 66, 1837–1844.
- Bertolero, M.A., Yeo, B.T.T., Bassett, D.S., D'Esposito, M., 2018. A mechanistic model of connector hubs, modularity and cognition. *Nat. Hum. Behav.* 2, 765–777.
- Bikbaev, A., Frischknecht, R., Heine, M., 2015. Brain extracellular matrix retains connectivity in neuronal networks. *Sci. Rep.* 5, 14527.
- Braak, H., Braak, E., 1991. Neuropathological staging of Alzheimer-related changes. *Acta Neuropathol.* 82, 239–259.
- Buckner, R.L., Sepulcre, J., Talukdar, T., Krienen, F.M., Liu, H., Hedden, T., Andrews-Hanna, J.R., Sperling, R.A., Johnson, K.A., 2009. Cortical hubs revealed by intrinsic functional connectivity: mapping, assessment of stability, and relation to Alzheimer's disease. *J. Neurosci.* 29, 1860.
- Cirrito, J.R., Yamada, K.A., Finn, M.B., Sloviter, R.S., Bales, K.R., May, P.C., Schoepp, D.D., Paul, S.M., Mennerick, S., Holtzman, D.M., 2005. Synaptic activity regulates interstitial fluid amyloid-beta levels in vivo. *Neuron* 48, 913–922.
- Colclough, G.L., Woolrich, M.W., Harrison, S.J., Rojas Lopez, P.A., Valdes-Sosa, P.A., Smith, S.M., 2018. Multi-subject hierarchical inverse covariance modelling improves estimation of functional brain networks. *Neuroimage* 178, 370–384.
- Du, J., Younes, L., Qiu, A., 2011. Whole brain diffeomorphic metric mapping via integration of sulcal and gyral curves, cortical surfaces, and images. *Neuroimage* 56, 162–173.
- Eisenstein, S.A., Koller, J.M., Piccirillo, M., Kim, A., Antenor-Dorsey, J.A., Videen, T.O., Snyder, A.Z., Karimi, M., Moerlein, S.M., Black, K.J., Perlmuter, J.S., Hershey, T., 2012. Characterization of extrastriatal D2 in vivo specific binding of [18 F](N-methyl)benperidol using PET. *Synapse* 66, 770–780.

- Elman, J.A., Madison, C.M., Baker, S.L., Vogel, J.W., Marks, S.M., Crowley, S., O'Neil, J.P., Jagust, W.J., 2014. Effects of beta-amyloid on resting state functional connectivity within and between networks reflect known patterns of regional vulnerability. *Cerebral Cortex* 26, 695–707.
- Fischl, B., Salat, D.H., Busa, E., Albert, M., Dieterich, M., Haselgrove, C., van der Kouwe, A., Killiany, R., Kennedy, D., Klaveness, S., Montillo, A., Makris, N., Rosen, B., Dale, A.M., 2002. Whole brain segmentation: automated labeling of neuroanatomical structures in the human brain. *Neuron* 33, 341–355.
- Greve, D.N., Fischl, B., 2009. Accurate and robust brain image alignment using boundary-based registration. *Neuroimage* 48, 63–72.
- Hahn, A., Strandberg, T.O., Stomrud, E., Nilsson, M., van Westen, D., Palmqvist, S., Ossenkoppele, R., Hansson, O., 2019. Association between earliest amyloid uptake and functional connectivity in cognitively unimpaired elderly. *Cereb. Cortex* 29, 2173–2182.
- Hajnal, J.V., Saeed, N., Soar, E.J., Oatridge, A., Young, I.R., Bydder, G.M., 1995. A registration and interpolation procedure for subvoxel matching of serially acquired MR images. *J. Comput. Assist. Tomogr.* 19, 289–296.
- Jack Jr., C.R., Lowe, V.J., Weigand, S.D., Wiste, H.J., Senjem, M.L., Knopman, D.S., Shiung, M.M., Gunter, J.L., Boeve, B.F., Kemp, B.J., Weiner, M., Petersen, R.C., 2009. Serial PIB and MRI in normal, mild cognitive impairment and Alzheimer's disease: implications for sequence of pathological events in Alzheimer's disease. *Brain* 132, 1355–1365.
- Jagust, W.J., Mormino, E.C., 2011. Lifespan brain activity, β -amyloid, and Alzheimer's disease. *Trends Cogn. Sci. (Regul. Ed.)* 15, 520–526.
- Jones, D.T., Knopman, D.S., Gunter, J.L., Graff-Radford, J., Vemuri, P., Boeve, B.F., Petersen, R.C., Weiner, M.W., Jack Jr., C.R., 2016. Cascading network failure across the Alzheimer's disease spectrum. *Brain* 139, 547–562.
- Joshi, A., Koeppe, R.A., Fessler, J.A., 2009. Reducing between scanner differences in multi-center PET studies. *Neuroimage* 46, 154–159.
- Karran, E., Mercken, M., Strooper, B.D., 2011. The amyloid cascade hypothesis for Alzheimer's disease: an appraisal for the development of therapeutics. *Nat. Rev. Drug Discov.* 10, 698–712.
- LaMontagne, P.J., Benzinger, T.L., Morris, J.C., Keefe, S., Hornbeck, R., Xiong, C., Grant, E., Hassenstab, J., Moulder, K., Vlassenko, A.G., Raichle, M.E., Cruchaga, C., Marcus, D., 2019. OASIS-3: longitudinal neuroimaging, clinical, and cognitive dataset for normal aging and Alzheimer disease. medRxiv, 2019.2012.2013.19014902.
- Lim, H.K., Nebes, R., Snitz, B., Cohen, A., Mathis, C., Price, J., Weissfeld, L., Klunk, W., Aizenstein, H.J., 2014. Regional amyloid burden and intrinsic connectivity networks in cognitively normal elderly subjects. *Brain* 137, 3327–3338.
- Moffat, G., Zhukovsky, P., Coughlan, G., Voineskos, A.N., 2022. Unravelling the relationship between amyloid accumulation and brain network function in normal aging and very mild cognitive decline: a longitudinal analysis. *Brain Commun.* 4, fcac282.
- Mormino, E.C., Smiljic, A., Hayenga, A.O., Onami, H., S. Greicius, M.D., Rabinovici, G.D., Janabi, M., Baker, S.L., Yen, V., I. Madison, C.M., Miller, B.L., Jagust, W.J., 2011. Relationships between beta-amyloid and functional connectivity in different components of the default mode network in aging. *Cerebr. Cortex* 21, 2399–2407.
- Mutlu, J., Landeau, B., Gaubert, M., de La Sayette, V., Desgranges, B., Chételat, G., 2017. Distinct influence of specific versus global connectivity on the different Alzheimer's disease biomarkers. *Brain* 140, 3317–3328.
- Nitsch, R.M., Farber, S.A., Growdon, J.H., Wurtman, R.J., 1993. Release of amyloid beta-protein precursor derivatives by electrical depolarization of rat hippocampal slices. *Proc. Natl. Acad. Sci. U.S.A.* 90, 5191–5193.
- Palmqvist, S., Schöll, M., Strandberg, O., Mattsson, N., Stomrud, E., Zetterberg, H., Blennow, K., Landau, S., Jagust, W., Hansson, O., 2017. Earliest accumulation of β -amyloid occurs within the default-mode network and concurrently affects brain connectivity. *Nat. Commun.* 8, 1214.
- Power, J.D., Schlaggar, B.L., Lessov-Schlaggar, C.N., Petersen, S.E., 2013. Evidence for hubs in human functional brain networks. *Neuron* 79, 798–813.
- Price, J.L., Morris, J.C., 1999. Tangles and plaques in nondemented aging and "preclinical" Alzheimer's disease. *Ann. Neurol.* 45, 358–368.
- Qiu, C., Bäckman, L., Winblad, B., Agüero-Torres, H., Fratiglioni, L., 2001. The influence of education on clinically diagnosed dementia incidence and mortality data from the Kungsholmen Project. *Arch. Neurol.* 58 (12), 2034–2039.
- Qiu, A., Lee, A., Tan, M., Chung, M.K., 2015. Manifold learning on brain functional networks in aging. *Med. Image Anal.* 20, 52–60.
- Quattromani, M.J., Hakon, J., Rauch, U., Bauer, A.Q., Wieloch, T., 2018. Changes in resting-state functional connectivity after stroke in a mouse brain lacking extracellular matrix components. *Neurobiol. Dis.* 112, 91–105.
- Quigley, H., Colloby, S.J., O'Brien, J.T., 2011. PET imaging of brain amyloid in dementia: a review. *Int. J. Geriatr. Psychiatry* 26, 991–999.
- Rahman, M.M., Lendel, C., 2021. Extracellular protein components of amyloid plaques and their roles in Alzheimer's disease pathology. *Mol. Neurodegener.* 16, 59.
- Rodrigue, K., Kennedy, K., Devous, M., Rieck, J., Hebrank, A., Diaz-Arrastia, R., Mathews, D., Park, D., 2012. β -Amyloid burden in healthy aging: regional distribution and cognitive consequences. *Neurology* 78, 387–395.
- Rousset, O.G., Collins, D.L., Rahmim, A., Wong, D.F., 2008. Design and implementation of an automated partial volume correction in PET: application to dopamine receptor quantification in the normal human striatum. *J. Nucl. Med.* 49, 1097–1106.
- Rousset, O.G., Ma, Y., Evans, A.C., 1998. Correction for partial volume effects in PET: principle and validation. *J. Nucl. Med.* 39, 904–911.
- Rowland, D.J., Garbow, J.R., Laforest, R., Snyder, A.Z., 2005. Registration of [18F]FDG microPET and small-animal MRI. *Nucl. Med. Biol.* 32, 567–572.
- Ritchie, J., Cox, S.R., Shen, X., Lombardo, M.V., Reus, L.M., Alloza, C., Harris, M.A., Alderson, H.L., Hunter, S., Neilson, E., Liewald, D.C.M., Auyeung, B., Whalley, H.C., Lawrie, S.M., Gale, C.R., Bastin, M.E., McIntosh, A.M., Deary, I.J., 2018. Sex Differences in the adult human brain: Evidence from 5216 UK biobank participants. *Cerebral Cortex* 28 (8), 2959–2975.
- Shen, X., Tokoglu, F., Papademetris, X., Constable, R.T., 2013. Groupwise whole-brain parcellation from resting-state fMRI data for network node identification. *Neuroimage* 82, 403–415.
- Sintini, I., Graff-Radford, J., Jones, D.T., Botha, H., Martin, P.R., Machulda, M.M., Schwarz, C.G., Senjem, M.L., Gunter, J.L., Jack Jr, C.R., Lowe, V.J., Josephs, K.A., Whitwell, J.L., 2020. Tau and amyloid relationships with resting-state functional connectivity in atypical Alzheimer's disease. *Cerebr. Cortex* 31, 1693–1706.
- Smith, S.M., Jenkinson, M., Woolrich, M.W., Beckmann, C.F., Behrens, T.E.J., Johansen-Berg, H., Bannister, P.R., De Luca, M., Drobnjak, I., Flitney, D.E., Niazy, R.K., Saunders, J., Vickers, J., Zhang, Y., De Stefano, N., Brady, J.M., Matthews, P.M., 2004. Advances in functional and structural MR image analysis and implementation as FSL. *Neuroimage* S208–S219 Academic Press.
- Sojkova, J., Zhou, Y., An, Y., Kraut, M.A., Ferrucci, L., Wong, D.F., Resnick, S.M., 2011. Longitudinal patterns of β -amyloid deposition in nondemented older adults. *Arch. Neurol.* 68, 644–649.
- Su, Y., Blazey, T.M., Owen, C.J., Christensen, J.J., Friedrichsen, K., Joseph-Mathurin, N., Wang, Q., Hornbeck, R.C., Ances, B.M., Snyder, A.Z., Cash, L.A., Koeppe, R.A., Klunk, W.E., Galasko, D., Brickman, A.M., McDade, E., Ringman, J.M., Thompson, P.M., Saykin, A.J., Ghetti, B., Sperling, R.A., Johnson, K.A., Salloway, S.P., Schofield, P.R., Masters, C.L., Villemagne, V.L., Fox, N.C., Förster, S., Chen, K., Reiman, E.M., Xiong, C., Marcus, D.S., Weiner, M.W., Morris, J.C., Bateman, R.J., Benzinger, T.L., 2016. Quantitative amyloid imaging in autosomal dominant Alzheimer's disease: results from the DIAN study group. *PLoS One* 11, e0152082.
- Su, Y., Blazey, T.M., Snyder, A.Z., Raichle, M.E., Marcus, D.S., Ances, B.M., Bateman, R.J., Cairns, N.J., Aldea, P., Cash, L., Christensen, J.J., Friedrichsen, K., Hornbeck, R.C., Farrar, A.M., Owen, C.J., Mayeux, R., Brickman, A.M., Klunk, W., Price, J.C., Thompson, P.M., Ghetti, B., Saykin, A.J., Sperling, R.A., Johnson, K.A., Schofield, P.R., Buckles, V., Morris, J.C., Benzinger, T.L.S., 2015. Partial volume correction in quantitative amyloid imaging. *Neuroimage* 107, 55–64.
- Su, Y., D'Angelo, G.M., Vlassenko, A.G., Zhou, G., Snyder, A.Z., Marcus, D.S., Blazey, T.M., Christensen, J.J., Vora, S., Morris, J.C., Mintun, M.A., Benzinger, T.L.S., 2013. Quantitative analysis of PiB-PET with FreeSurfer ROIs. *PLoS ONE* 8, e73377.
- Sun, Y., Xu, S., Jiang, M., Liu, X., Yang, L., Bai, Z., Yang, Q., 2021. Role of the extracellular matrix in Alzheimer's disease. *Front. Aging Neurosci.* 13, 707466.
- Tan, M., Qiu, A., 2016. Large deformation multiresolution diffeomorphic metric mapping for multiresolution cortical surfaces: a coarse-to-fine approach. *IEEE Trans. Image Process* 25, 4061–4074.
- Thal, D.R., Rüb, U., Orantes, M., Braak, H., 2002. Phases of A β -deposition in the human brain and its relevance for the development of AD. *Neurology* 58, 1791–1800.
- Tomasi, D., Volkow, N.D., 2012. Aging and functional brain networks. *Mol. Psychiatry* 17, 549–558.
- van den Heuvel, M.P., Sporns, O., 2013. Network hubs in the human brain. *Trends Cogn. Sci.* 17, 683–696.
- Villain, N., Chételat, G., Grasset, B., Bourgeat, P., Jones, G., Ellis, K.A., Ames, D., Martins, R.N., Eustache, F., Salvado, O., Masters, C.L., Rowe, C.C., Villemagne, V.L., 2012. Regional dynamics of amyloid- β deposition in healthy elderly, mild cognitive impairment and Alzheimer's disease: a voxelwise PiB-PET longitudinal study. *Brain* 135, 2126–2139.
- Villemagne, V.L., Pike, K.E., Chételat, G., Ellis, K.A., Mulligan, R.S., Bourgeat, P., Ackermann, U., Jones, G., Szoëke, C., Salvado, O., Martins, R., O'Keefe, G., Mathis, C.A., Klunk, W.E., Ames, D., Masters, C.L., Rowe, C.C., 2011. Longitudinal assessment of A β and cognition in aging and Alzheimer disease. *Ann. Neurol.* 69, 181–192.
- Yeo, B.T., Krienen, F.M., Sepulcre, J., Sabuncu, M.R., Lashkari, D., Hollinshead, M., Roffman, J.L., Smoller, J.W., Zöllei, L., Polimeni, J.R., Fischl, B., Liu, H., Buckner, R.L., 2011. The organization of the human cerebral cortex estimated by intrinsic functional connectivity. *J. Neurophysiol.* 106, 1125–1165.
- Zhong, J., Qiu, A., 2010. Multi-manifold diffeomorphic metric mapping for aligning cortical hemispheric surfaces. *Neuroimage* 49, 355–365.